Available online at www.sciencedirect.com
ScienceDirect
Energy Reports 8 (2022) 588–596
www.elsevier.com/locate/egyr

2022 The 4th International Conference on Clean Energy and Electrical Systems (CEES 2022), 2–4 April, 2022, Tokyo, Japan

Red deer algorithm based selective harmonic elimination for renewable energy application with unequal DC sources

Yasin Bektaş[a], Hulusi Karaca[b,*]

[a] Aksaray University, Technical Sciences Vocational High School Department of Electrical-Energy, Aksaray, Turkey
[b] Selçuk University, Technology Faculty, Electrical-Electronics Engineering, Konya, Turkey

Received 9 May 2022; accepted 19 May 2022
Available online xxxx

Abstract

This study aims to find the optimal switching angles in a cascaded H-bridge multilevel inverter (CHB-MLI) fed by photovoltaic (PV) panels, keeping the output voltage constant regardless of the panel voltage change and eliminating low-order harmonics. For this purpose, Red Deer Algorithm (RDA), a newly developed algorithm, has been applied to solve selective harmonic elimination (SHE) equations. Calculated switching angles are simulated by applying three-phase 7-level CHB-MLI in Matlab/Simulink environment. RDA optimization has been compared in performance to evolutionary algorithms such as particle swarm optimization (PSO), genetic algorithm (GA) and pigeon inspired optimization (PIO). The results show that in the case of unequal DC voltage, RDA can suppress selected harmonics accurately and quickly while controlling the fundamental voltage with a 0.02% error. The proposed RDA optimization can be used for multilevel inverters fed by any number of variable input voltages to eliminate selected harmonics and reduce total harmonic distortion (THD) without complex analytical calculations.

Peer-review under responsibility of the scientific committee of the 4th International Conference on Clean Energy and Electrical Systems, CEES, 2022.

Keywords: Red Deer Algorithm (RDA); Selective harmonic elimination (SHE); Multilevel inverter (MLI); Unequal DC sources; Renewable energy

1. Introduction

Considering the recent trends, it is evident that renewable energy sources will be an essential part of the future of electricity generation due to environmental problems and increasing fuel prices. Different renewable energy sources such as solar energy, wind energy, and geothermal energy are equipment for generating electrical energy. Solar power is a good option for the electric age among renewable energies because of its accessibility and cleanliness. Solar energy is directly converted to DC power by photovoltaic (PV) cells. While solar panel efficiency is usually around 15%–20%, solar cell efficiency can reach up to 42% in some cases [1]. The output power of PV modules can vary depending on the conditions of the modules, such as temperature, solar radiation, cell size, and load [2]. In

* Corresponding author.
E-mail address: hkaraca@selcuk.edu.tr (H. Karaca).

https://doi.org/10.1016/j.egyr.2022.05.209

Peer-review under responsibility of the scientific committee of the 4th International Conference on Clean Energy and Electrical Systems, CEES, 2022.

grid-connected systems [3], there is a need for DC/AC converters, i.e., inverters, AC mains, and supplying AC load in off-grid systems. Traditional two-level inverters are mostly used in small-scale industries and utility applications [4]. However, the output of this inverter contains more harmonics, so expensive and bulky low-pass passive filters must be used before powering the grid. In addition, high voltage stress and high switching loss prevent the application of these inverters in high power applications [5]. Therefore, in the case of high-power demand from solar energy, it is necessary to have a multi-level inverter. There are different topologies as Cascaded H-Bridge MLI (CHB-MLI), Diode Clamped MLI (DC-MLI), and Capacitor Clamped MLI (CC-MLI). Among these, CHB-MLI has been accepted as the most suitable topology for PV systems due to its fault tolerance, modular and robust structure, and allowing equal and unequal DC usage [6].

As a result of the development of new MLI topologies, difficulties have emerged in these inverters' control and modulation techniques. Some low order dominant harmonics in the stepped output voltage waveform produced by MLI is a critical problem to solve. The main effects of these harmonics are voltage rippling, loss increase, malfunction. These harmonics also affect the power quality. Although there are many control and modulation methods, the modulation method that overcomes the mentioned problems is selective harmonic elimination (SHE) or programmed PWM technique.

In the SHE-PWM technique, first, the fundamental component of the output voltage is determined. A set of equations are then created for the undesirable/selected harmonics and set equal to zero. Then, analytical solutions of these equations are sought to determine the switching angles. The principle is simple, but these equations contain many trigonometric functions and can have more than one set of solutions. Therefore, the solution to the problem is very complex.

The methods used in the SHE problems may be classified into three categories: (i) numerical methods, (ii) algebraic methods, and (iii) meta-heuristic algorithms. The first two methods have several limitations, so researchers turned to metaheuristic algorithms.

Algorithms such as Genetic Algorithm (GA) [7–9], Particle Swarm Optimization (PSO) [9], and Whale Optimization Technique are meta-heuristics algorithms used to solve SHE equations [10].

Each algorithm cannot find a solution for all modulation indexes. Therefore, researchers focus on new optimization methods. Also, most of the methods used to solve the SHE equations assume that the DC sources are all equal. However, in some practical situations, for example, in renewable energy applications such as solar panel and fuel cell applications [11], variation of dc sources will seriously impact the overall THD and therefore needs to be considered.

For this purpose, a relatively new Red Deer Algorithm (RDA) optimization, which can solve the SHE problem in the presence of varying input voltages in the CHB MLI fed by the PV panels, is adapted to solve the SHE equations. It is a much faster and more robust algorithm than its counterparts such as PIO [12], GA, PSO, and GSA. The simulation results show that the RDA technique can be effectively applied to MLIs.

2. Cascaded H-bridge inverters

The circuit diagram of the 7-level single-phase CHB-MLI is shown in Fig. 1a. As can be seen, the MLI consists of series-connected H-bridge inverters, each powered by an isolated discrete DC source. The output waveform for a single phase is shown in Fig. 1b. The output voltage level can be expressed as N=2k+1, where k is the number of sources. Accordingly, 7-level CHB-MLI three h-bridges and separate dc sources are needed. Depending on the application, a three-phase structure is formed by connecting the outputs of three single-phase multilevel inverters as Y (star) or Δ (delta).

3. Selective harmonic elimination problem in multilevel inverters

The switching angles at the fundamental frequency in the SHE equations are obtained by solving such that the fundamental voltage is obtained as desired and the undesirable/selected lower order harmonics are eliminated. A single switching is made for each module in a loop to reduce switching losses and provide better electromagnetic interference (EMI). Therefore, the number of switching angles equals the number of individual DC sources (k). With k being the number of switching, k-1 low-order harmonics can be eliminated from the inverter output voltage.

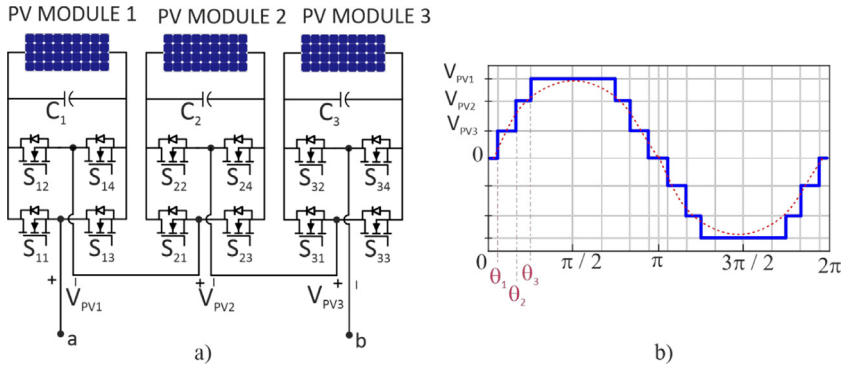

Fig. 1. Single-phase 7-level CHB-MLI (a) circuit structure (b) output voltage waveform.

The Fourier expansion of the output voltage can explain the nonlinear harmonic equations required to obtain optimal switching angles in 7-level CHB-MLI. The expression of the output voltage including all harmonic components can be defined as in (1) [8]

$$V_{ab}(\omega t) = \sum_{(odd)n=1,3,\ldots}^{\infty} \frac{4}{\pi n}[V_{PV1}\cos(n\theta_1) + V_{PV2}\cos(n\theta_2) + V_{PV3}\cos(n\theta_3)]\sin(\omega t) \tag{1}$$

where, V_{PV1}, $V_{PV2,}$ and V_{PV3} are the input DC voltages (PV panel voltage). θ_1, θ_2, and θ_3 are the switching angles and they must satisfy the condition $0 \leq \theta_1 \leq \theta_2 \leq \theta_3 \leq \pi/2$.

The third harmonic component and multiples of the third harmonic at phase-to-phase voltages can be neglected in a balanced three-phase system. Therefore, it is sufficient to eliminate 5th, 7th, 11th, etc., harmonic orders in the line voltage waveform at the low switching frequency. If the set of equations is rearranged as follows:

$$\begin{aligned} V_{fund} &= V_{PV1}\cos(\theta_1) + V_{PV2}\cos(\theta_2) + V_{PV3}\cos(\theta_3) \\ V_{5^{th}} &= V_{PV1}\cos(5\theta_1) + V_{PV2}\cos(5\theta_2) + V_{PV3}\cos(5\theta_3) \\ V_{7^{th}} &= V_{PV1}\cos(7\theta_1) + V_{PV2}\cos(7\theta_2) + V_{PV3}\cos(7\theta_3) \end{aligned} \tag{2}$$

The first of the SHE equations is used to control the amplitude of the fundamental waveform, as seen in (2). Other equations are set zero to eliminate the selected harmonics. Then, these equations are solved by a proper method. The purpose here is to keep the voltage value at the fundamental frequency at the desired value and to eliminate or minimize the low-order harmonics (V_5, V_7, etc.). This paper proposes an RDA optimization method to obtain the best possible solutions for SHE equations.

In three-phase systems, the THD value can be calculated like Eq. (3). The same formula is used for the THD_e value, and it is calculated up to the 7th harmonic.

$$THD = \frac{\sqrt{V_5^2 + V_7^2 + V_{11}^2 + \cdots}}{|V_1|} \tag{3}$$

3.1. Problem formulation of selective harmonic elimination using RDA

The fitness function (FF) is given in (4). To eliminate harmonics, each term of the function f must be equal to zero, where $\theta_1, \theta_2, \ldots, \theta_k$ are the switching angles. Where V_{ref} is the desired reference voltage. ε given in (5) is the acceptable error tolerance, and $\varepsilon = 1$ V error can be considered the solution for this study.

$$f = \min_{\theta_i}\left\{\left|V_{fund} - V_{ref}\right| + \left(\left|V_{5^{th}}\right|^2 + \left|V_{7^{th}}\right|^2\right)\right\} = 0, \quad 0 \leq \theta_1 < \theta_2 < \theta_3 \leq \pi/2 \tag{4}$$

$$V_{fund} - V_{ref} \leq \varepsilon \tag{5}$$

4. RDA optimization

Red Deer Optimization (RDA) [13] was first introduced in 2016. Subsequently, a new RDA optimization approach is introduced [14]. The peculiar mating behavior of the Scottish Red Deer during the breeding season was the main inspiration for this metaheuristic algorithm. RDA, like other techniques, begins with a random population of red deer (RDs). The best RDs in the population are chosen and referred to as "RD male", while the rest are referred to as "hinds". First of all, the RD male must roar. Depending on the strength of the roaring stage, male deer are divided into two groups as commanders and single male deer (stags). After the roaring stage, the commanders and the stags fight for their harems. A stag can become a commander if he wins the fight. After the combat process, harems are made up of commanders only. The roar of commanders and their skills in the combat phase are closely related to the number of hinds in their harems. As a result, the commanders mate a series of hints in their harems. In addition, each commander can mate with a certain proportion of hints in other harems. The stags mate with the nearest hint, regardless of the harem limitation. This step also covers the exploration and concentration phases. Another critical step in optimizing RDA is the mating process in which RDs are formed from the offspring. At this stage, new solutions to optimization problems are generated. Finally, the next generation of the algorithm is produced by giving a chance to evolutionarily weak solutions [14].

4.1. RDA algorithm in solving SHEPWM

(a) *Creation of the initial population:* A set of variables is created to be optimized. A "*Red Deer*" corresponds to a suitable solution X within the solution space. The optimization problem can be expressed in terms of dimensions as follows.

$$Value = f(Red\ Deer) = f(X_1, X_2, X_3, \ldots, X_{N_{var}}) \tag{6}$$

where, X_{Nvar} specifies the size of the array, while X_1, X_2, and X_3, etc., specify the array's components. In this study, X_{Nvar} is taken as 50. For each array component (i.e., RD), a location is assigned based on the size of the problem. Since there are three variables for a 7-level CHB, variables are assigned for each RD as in (7). The position of the ith deer is defined as follows:

$$X_i = [\theta_1, \theta_2, \theta_3] = for\ i = 1, 2, 3, \ldots, X_{N_{var}} \tag{7}$$

RDA works on a population of solutions to a particular problem rather than an individual solution. So, it starts randomly. In this algorithm, the position of the best male RD found will be the solution to the problem. Fig. 2(a) shows the randomly generated RD population for 7-level CHB-MLI.

(b) *Roaring*: Regarding the resolution space in the roar stage, the male RD has neighbors, and each male RD is allowed to change his position. As a result of this change, whichever of the previous and subsequent positions has the better fitness function (*FF*) value is selected. The following equation is used to update the position of male RDs.

$$male_{new} = \begin{cases} male_{old} + a_1 \times (((UB - LB) * a_2) + LB), & if\ a_3 \geq 0.5 \\ male_{old} - a_1 \times (((UB - LB) * a_2) + LB), & if\ a_3 < 0.5 \end{cases} \tag{8}$$

where, $male_{new}$ represents the new position of male deers, $male_{old}$ its old position, and UB and LB are the upper and lower limits of the search area, respectively. a_1, a_2, and a_3 are randomly chosen with a uniform distribution between zero and one. Two situations arise based on the solution space, as depicted in Fig. 2(b). The B* state in the *FF* is considered as the new location because it is better than the previous location, while the A* location is not accepted as the new location because it is worse than the previous location. A male RD that succeeds in a roar is considered a commander, while a male RD that fails is considered a stag.

(c) *Fight*: Every commander is allowed to fight with random stags. Regarding the fighting process, the two mathematical formulas are provided as:

$$New1 = \frac{(Com + Stag)}{2} + b_1 \times (((UB - LB) * b_2) + LB) \tag{9}$$

$$New2 = \frac{(Com + Stag)}{2} - b_1 \times (((UB - LB) * b_2) + LB) \tag{10}$$

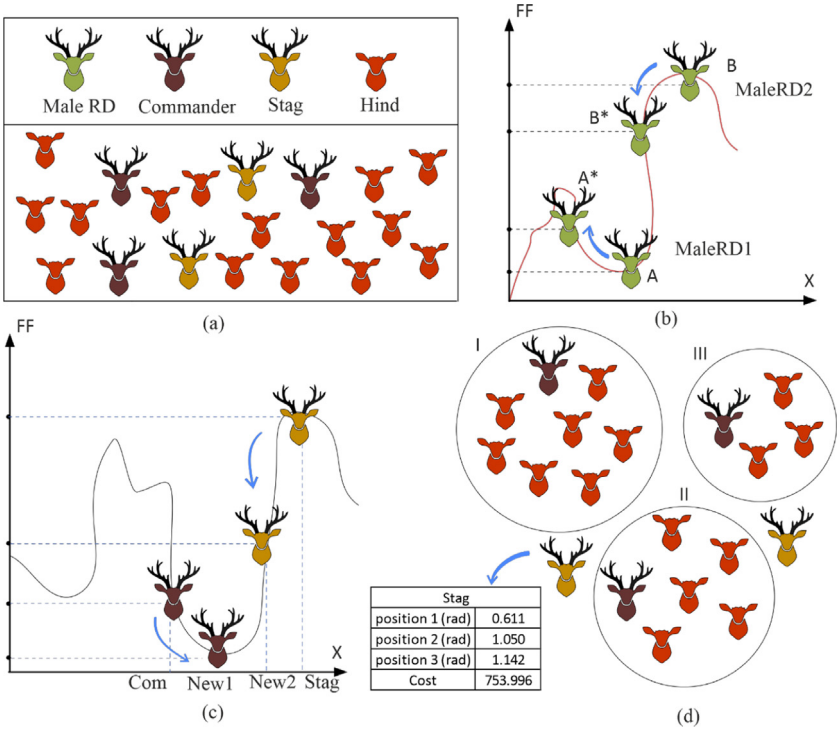

Fig. 2. Stages of RDA (a) Population of RD (b) Roaring process (c) Fighting process (d) Harems.

b_1 and b_2 are randomly chosen with a uniform distribution between zero and one due to the randomness of the fighting process. Regarding the resolution area, a commander and a stag are allowed to approach each other. Commander (*Com*), single male RD (*Stag*), *New1* (new status1), *New2* (new status2), whichever of the four solutions has the better *FF* is appointed as the new commander. It simply illustrates this procedure in Fig. 2(c). As seen in this figure, the *FF* value of *New1* is better than the others. In this case, the commander remains commander, and his new position is *New1*. The commander won the fight and the stag lost.

(d) *Creation phase of harems:* After the roaring and fighting phase comes forming the harems. A harem consists of a male commander and a group of female deer (hinds). The number of hinds in harems depends on the commander's roar and fighting ability. The power of the commander is defined in proportion to how much it provides the *FF* value. The number of hinds in harems is determined as follows:

$$N.\text{harem}_n = \text{round}\{P_n.N_{\text{hind}}\} \tag{11}$$

where $N.\text{harem}_n$ is the number of hinds in the nth harem, N_{hind} is the number of all hinds, and P_n is the commander's power in the nth harem. The formed harem I, II, and III are shown in Fig. 2(d), the commander in the 1st harem has the most hinds because he was more successful than the others in the roaring and fighting process. Stags are not included in the harem.

(e) *Mating phase:* The mating phase occurs in three different situations. In the first, the commander of each harem mates with $\alpha\%$ of the hinds in his harem. In the second, any commander mates with hinds of other harems. Here, a random harem is selected, and the commander in this harem mates with $\beta\%$ of the hinds in other harems. He attacks another harem to expand his command area. β is an initial parameter for the algorithm model. The range value of this parameter is between zero and one. In the third case, each stag mates with the closest female RD, regardless of harem restrictions.

(f) *Creation of offspring:* In all three cases, offspring are produced by the procedure in (12) during the mating phase.

$$offs = \frac{(Com + Hind)}{2} + (UB - LB) \times c \tag{12}$$

where, *offs* is the new offspring RD; that is, it represents a new solution. c is randomly generated between zero and one. For the third case in the mating phase, Com in (12) will be replaced with Stag.

(g) *Selection of the new generation:* Two different strategies are followed to select the next generation. In the first, the best of all male RDs (Commanders and Stags) are stored (a certain percentage of the best solutions). In the second strategy, hinds are selected for the next generation from among all hinds and offspring produced during the mating phase, using the fitness tournament or roulette wheel mechanism. The next generation is produced with the selected male and female RDs.

(h) *Stop criterion:* The stopping condition can be the iteration count, the best solution ever found, or a time interval. For RDA-based SHE PWM, the number of iterations is taken as the stopping criterion. Steps b–h are repeated until the stopping criterion is met.

Table 1 shows the parameter values for RDA. Where α, β, γ values are used to control the intensification and diversification areas. These three parameter values are between zero and one. By changing these values randomly, the algorithm is run many times, and the best results are written in Table 1. The other values are similarly adjusted by trial and error so that the RDA can best solve the SHE.

Initially, a series of DC voltages V_{PV1}, V_{PV2}, and V_{PV3} are selected, and then RDA is applied. While satisfying the constraints given above, an optimal switching angle combination [θ_1, θ_2, θ_3] will be found with the minimum THD at the end of the simulation.

Table 1. Parameters of RDA.

Parameters	Value	Parameters	Value	Parameters	Value
Number of variables	5	Number of Hinds	44	Roar	0.2
Iteration number	50	Alfa (α)	1.0	Fight	0.5
Number of the population	50	Beta (β)	0.6	Mating	0.8
Number of MaleRD	6	Gama (γ)	0.5		

5. Simulation results

RDA optimization is programmed as an m-file in MATLAB to obtain optimum switching angles. The calculated switching angles are applied to the CHB-MLI. In this study, the voltages have been randomly varied between 50–60 V with 1 V precision to create different combinations. The input voltages and the angles obtained with PIO, GA, PSO, and RDA is given in Table 2.

Table 2. Angles obtained with PIO, GA, PSO, and RDA.

NO	Input voltages (V)	Output angles using RDA	Output angles using PIO [12]	Output angles using PSO [12]	Output angles using GA [12]
	[V_1 to V_3]	[θ_1 to θ_3]	[θ_1 to θ_3]	[θ_1 to θ_3]	[θ_1 to θ_3]
1	[50 50 53]	[11.92 27.49 56.51]	[11.87 27.93 56.76]	[11.66 28.18 56.69]	[11.95 27.59 56.61]
2	[50 52 51]	[11.27 28.42 57.03]	[11.34 27.60 56.54]	[11.00 28.47 57.48]	[11.25 28.88 57.31]
3	[50 53 57]	[12.17 32.51 59.48]	[12.27 32.86 59.67]	[12.15 33.35 59.61]	[12.21 32.91 59.77]
4	[50 55 52]	[11.08 31.66 59.18]	[11.22 32.24 59.54]	[11.36 32.18 59.53]	[11.39 32.85 59.92]
5	[50 58 51]	[10.95 33.47 60.58]	[10.51 32.06 59.67]	[11.14 33.93 60.81]	[10.84 33.05 60.27]
6	[50 59 52]	[11.34 34.60 61.35]	[11.37 34.68 61.39]	[11.47 34.73 61.70]	[11.51 34.99 61.58]
7	[51 52 56]	[12.24 32.23 59.22]	[12.37 32.77 59.51]	[11.47 34.73 61.70]	[12.31 32.55 59.40]
8	[53 59 53]	[11.02 33.21 60.30]	[11.15 33.58 60.55]	[11.13 33.81 60.28]	[10.94 32.97 60.15]
9	[50 50 53]	[13.22 37.61 62.84]	[10.77 26.51 55.87]	[13.09 37.96 63.02]	[14.41 39.50 63.78]
10	[54 50 53]	[12.41 32.12 58.87]	[12.49 32.45 59.06]	[12.62 32.28 59.13]	[13.13 34.56 60.21]

As shown in Fig. 3, RDA reaches the global optimal solution in only 8 iterations, PIO reaches in 10 iterations, and PSO and GA more than 25 iterations. Thus, it can be seen from the results that RDA can reach the global optimum in a short time compared to other algorithms. The number of iterations and populations for all algorithms is 50. Table 3 was formed by taking the first ten of the 20 values calculated in [12]. Harmonic analyzes will be given only for the first case among the cases specified in Table 3.

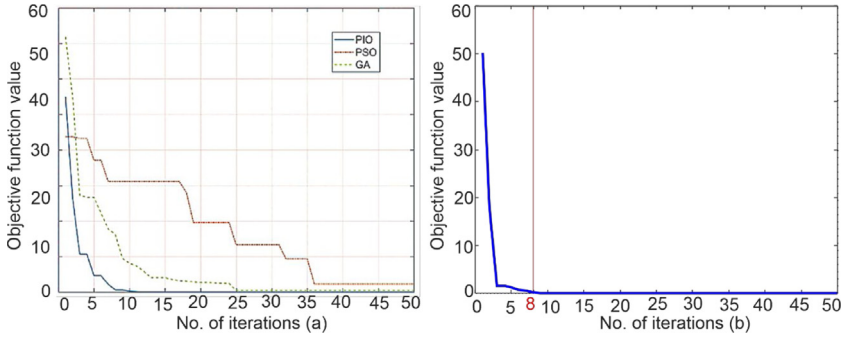

Fig. 3. Convergence rates of different algorithms a) PSO, GA, PIO [12] and b) RDA.

Table 3. Simulation results using PIO, PSO, GA [12], and RDA.

NO	Vout (rms)				Vout (error)				THD (line to line)				THDe (line to line)			
	RDA	PIO	PSO	GA	RDA	PIO	PSO	GA	RDA	PIO	PSO	GA	RDA	PIO	PSO	GA
1	**110.03**	109.74	109.74	109.96	**0.02**	0.23	0.23	0.04	**8.67**	8.74	8.87	8.66	**0.03**	0.03	0.24	0.06
2	**110.03**	110.66	109.74	109.67	**0.02**	0.60	0.23	0.30	**8.89**	8.71	8.86	9.02	**0.04**	0.05	0.46	0.03
3	**110.03**	109.74	109.53	109.60	**0.02**	0.23	0.43	0.36	**8.22**	8.07	8.06	8.02	**0.03**	0.04	0.43	0.11
4	**110.03**	109.46	109.53	108.97	**0.02**	0.49	0.43	0.94	**8.72**	8.45	8.44	8.19	**0.04**	0.04	0.16	0.03
5	**110.03**	111.44	109.60	110.45	**0.02**	1.31	0.36	0.41	**8.63**	8.73	8.69	8.51	**0.05**	0.03	0.07	0.05
6	**110.03**	109.96	109.74	109.67	**0.02**	0.04	0.23	0.30	**8.98**	8.99	9.16	9.08	**0.04**	0.04	0.29	0.05
7	**110.03**	109.46	109.74	109.74	**0.02**	0.49	0.23	0.23	**8.29**	8.07	8.16	8.14	**0.04**	0.04	0.46	0.04
8	**110.03**	109.67	109.74	110.24	**0.02**	0.30	0.23	0.22	**8.41**	8.48	8.28	8.36	**0.06**	0.03	0.39	0.04
9	**110.03**	120.92	109.74	108.05	**0.02**	9.92	0.23	1.78	**9.88**	8.61	10.05	10.95	**0.04**	0.03	0.35	0.04
10	**110.03**	109.74	109.74	109.96	**0.02**	0.30	0.23	1.97	**8.27**	8.13	8.10	7.75	**0.05**	0.02	0.24	0.04

Table 4. The number of function calls to reach the optimum value and computation time.

Optimization	Run number										AVG	Avg. time taken (0.1282*Fn calls) (sec)
	1	2	3	4	5	6	7	8	9	10		
RDA	1.069	1.14	1.132	1.161	1.216	1.151	1.188	1.124	1.108	1.138	1.14	0.146
PIO [12]	450	300	450	400	350	450	500	400	450	300	405	51.921
PSO [12]	1900	1400	550	750	1000	1250	1100	750	950	1650	1130	144.866
GA [12]	800	1400	750	850	950	1650	1750	1000	1250	1800	1220	156.404

Due to the nature of RDA, PIO, PSO, and GA heuristics, there is always the possibility of getting stuck in the local optimum. To verify that it has reached the global optimum, the number of calculated functions calls for PIO, PSO, and GA in [12], and the test results for the proposed RDA optimization are given in Table 4. The RDA algorithm was run ten times for the same input, and it was examined whether it converged to the global minimum. As seen in the table results, the fastest running algorithm is the proposed RDA algorithm. The time taken for each RDA function call is calculated on a computer running Intel Core - i7 processor @ 5.0 GHz and 16 GB of RAM.

In [12], the simulation results when the switching angles calculated with PIO, PSO, and GA and the switching angles calculated with RDA are applied for the first case ($V_{PV1} = 50$, $V_{PV2} = 50$, $V_{PV3} = 53$) are given in Figs. 4–7, respectively. The phase voltage waveform for RDA is shown in Fig. 4(a), the frequency spectrum for line voltage THD is shown in Fig. 4(b), and the frequency spectrum of THD_e is shown in Fig. 4(c). As seen in Fig. 4, when the switching angles calculated with RDA are applied, the fundamental voltage is 155.6 V peak (110.03 V rms), the THD value of the line voltage is 8.67%, and the THD_e value of the line voltage is 0.03%.

The phase voltage waveform for PIO is shown in Fig. 5(a), THD is shown in Fig. 5(b) and THD_e is shown in Fig. 5(c). As seen in Fig. 5, the fundamental voltage in PIO is 155.2 V peak (109.74 V rms), the THD value of the line voltage is 8.74%, and the THD_e value of the line voltage is 0.03%.

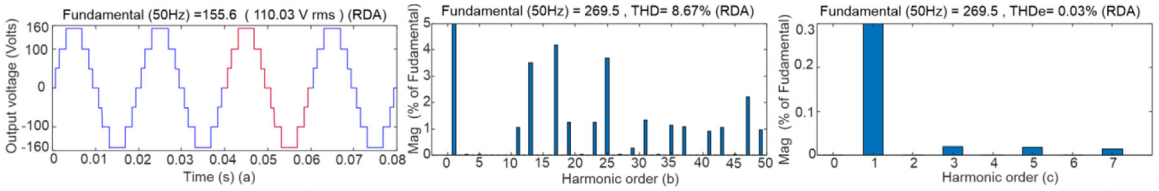

Fig. 4. For case 1 (RDA), a) output voltage waveform b) THD result (line to line) c) THD_e result (line to line).

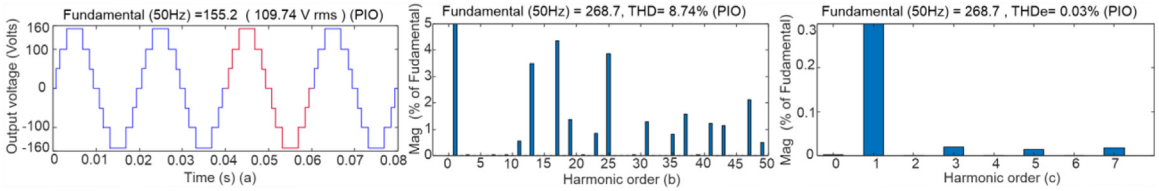

Fig. 5. For case 1 (PIO), a) output voltage waveform b) THD result (line to line) c) THD_e result (line to line).

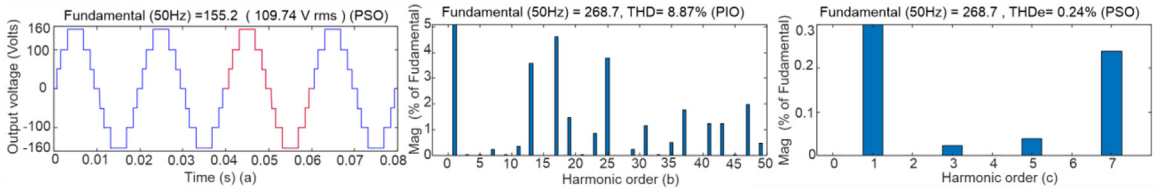

Fig. 6. For case 1 (PSO), a) output voltage waveform b) THD result (line to line) c) THD_e result (line to line).

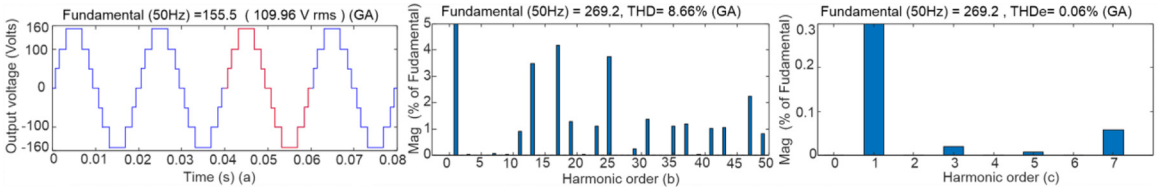

Fig. 7. For case 1 (GA), a) output voltage waveform b) THD result (line to line) c) THD_e result (line to line).

The phase voltage waveform for PSO is shown in Fig. 6(a), THD is shown in Fig. 6(b) and THD_e is shown in Fig. 6(c). As seen in Fig. 6, the fundamental voltage in PSO is 155.2 V peak (109.74 V rms), the THD value of the line voltage is 8.77%, and the THD_e value of the line voltage is 0.24%.

The phase voltage waveform for GA is shown in Fig. 7(a), the frequency spectrum for line voltage THD is shown in Fig. 7(b), and THD_e is shown in Fig. 7(c). As seen in Fig. 7, the fundamental voltage in GA is 155.5 V peak (109.9 V rms), the THD value of the line voltage is 8.66%, and the THD_e% value of the line voltage is 0.06%.

As shown in Table 3, the RDA produces the fundamental voltage with an error of 0.02%, which is much smaller than that of the PIO, PSO and GA algorithms. As a result, the RDA algorithm is the only algorithm that finds the fundamental voltage with more minor errors and suppresses the selected harmonics.

6. Conclusions

In this study, the relatively new RDA has been successfully applied to the switching angle optimization problem for the elimination of selected harmonics in CHB-MLI with unequal dc sources (PV panels). Simulation on three-phase 7-level CHB-MLI is provided to validate the theoretical analysis. It has been shown that the proposed method can generally produce better solutions when compared with the GA and PSO optimizations commonly used in the literature and the newly developed PIO optimization results. The results showed that the proposed method effectively

minimizes the selected harmonics, and the THD value can be reduced with very little error in the output voltage. Moreover, this method can be used for any number of voltage variations without complex analytical calculations.

Declaration of competing interest

The authors declare that they have no known competing financial interests or personal relationships that could have appeared to influence the work reported in this paper.

References

[1] Maghami MR, Hizam H, Gomes C, Radzi MA, Rezadad MI, Hajighorbani S. Power loss due to soiling on solar panel: A review. Renew Sustain Energy Rev 2016;59:1307–16, (2016).
[2] Alhaj Omar F, Kulaksiz AA. Experimental evaluation of a hybrid global maximum power tracking algorithm based on modified firefly and perturbation and observation algorithms. Neural Comput Applic 2021;33.24:17185–208, (2021).
[3] Venkata R. Vakacharla, et al. State-of-the-art power electronics systems for solar-to-grid integration. Sol Energy 2020;210:128–48, (2020).
[4] Keith Corzine, Familiant Yakov. A new cascaded multilevel H-bridge drive. IEEE Trans Power Electron 2002;17.1:125–31, (2002).
[5] Chris M. Hutson, Venayagamoorthy Ganesh K, Corzine Keith A. Optimal SVM switching for a multilevel multi-phase machine using modified discrete PSO. In: 2008 IEEE swarm intelligence symposium. IEEE; 2008, p. 1–6, (2008).
[6] Hari Priya Vemuganti, et al. A survey on reduced switch count multilevel inverters. IEEE Open J Ind Electron Soc 2021;2:80–111, (2021).
[7] Kaushal Bhatt, Chakravorty Sandeep. Mitigation of harmonics from output of cascaded H bridge multilevel inverter using SHE PWM and AI technique: A review. Recent Adv Electr Electron Eng (Formerly Recent Pat Electr Electron Eng) 2020;13.7:952–68, (2020).
[8] Enes Bektas, Karaca Hulusi. GA based selective harmonic elimination for multilevel inverter with reduced number of switches: an experimental study. Elektronika Elektrotechnika 2019;25.3:10–7, (2019).
[9] Aman Parkash, Shimi SL, Chatterji S. Harmonics reduction in cascade H-bridge multilevel inverters using GA and PSO. Int J Eng Trends Technol 2014;12.9:453–65, (2014).
[10] Aala Kalananda Vamsi Krishna Reddy, Venkata Lakshmi Narayana Komanapalli. Optimal total harmonic distortion minimization in multilevel inverter using improved whale optimization algorithm. Int J Emerg Electr Power Syst 2020;21.3. (2020).
[11] Prabhat Ranjan Bana, et al. Recently developed reduced switch multilevel inverter for renewable energy integration and drives application: topologies, comprehensive analysis and comparative evaluation. IEEE Access 2019;7:54888–909, (2019).
[12] Mahesh Aeidapu, Sandhu Kanwarjit Singh. Optimal switching angle scheme for a cascaded H bridge inverter using pigeon inspired optimization. Int J Emerg Electr Power Syst 2019;20.2. (2019).
[13] Fard AF, Hajiaghaei-Keshteli M. Red Deer Algorithm (RDA); a new optimization algorithm inspired by Red Deers' mating. In: International conference on industrial engineering. IEEE; 2016, p. 331–42, 12. (2016).
[14] Fathollahi-Fard, et al. Red deer algorithm (RDA): a new nature-inspired meta-heuristic. Soft Comput 2020;24.19:14637–65, (2020).